Ostracod palaeolimnological analysis reveals drastic historical changes in salinity, eutrophication and biodiversity loss in a coastal Mediterranean lake

J Marco-Barba, F Mesquita-Joanes and MR Miracle

The Holocene 2013 23: 556 originally published online 18 January 2013
DOI: 10.1177/0959683612466752

Research report

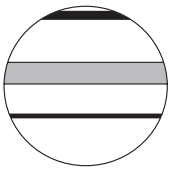

The Holocene
23(4) 556–567

DOI: 10.1177/0959683612466752
hol.sagepub.com

Ostracod palaeolimnological analysis reveals drastic historical changes in salinity, eutrophication and biodiversity loss in a coastal Mediterranean lake

J Marco-Barba,[1] F Mesquita-Joanes[1] and MR Miracle[1]

Abstract

The Albufera of Valencia, one of the largest oligohaline coastal lagoons of the Iberian Peninsula, has suffered hydrological and landscape modifications since medieval times. This paleolimnological study clears up the controversy about the factors, which drove the lake to its present state. Lithological descriptions, ostracod paleoassemblages and *Cyprideis torosa* (Jones, 1850) shell morphological variations and geochemistry ($\delta^{18}O$, $\delta^{13}C$ and Sr/Ca) have been used to reconstruct the lake ecosystem evolution during the last two centuries. The sandy sediments at the bottom of L'Antina core (63 cm) presented a typical assemblage of brackish water ostracods, with shell-derived $\delta^{18}O$ values, inferred salinity and Sr/Ca_{WATER} characteristic of waters with marine influence. However, 10 cm above, coinciding with a drastic change in lithology, ostracod palaeoassemblages and decreased shell $\delta^{18}O$ indicated a shift to freshwater influences. At the top of the sequence, inferred salinity suggests oligohaline waters and ostracods have almost disappeared. The early brackish conditions of Lake Albufera changed at the beginning of the 19th century when important hydrological modifications were undertaken for irrigation and started the major period of rice field expansion. Later, with the change of traditional rice farming to a more technological agriculture, together with increased domestic and industrial sewage inputs, the Albufera became a highly eutrophicated system 50 years ago. Eventually, the loss of macrophyte cover, cyanobacteria blooms and the increase of grazing by fish forced the loss of ostracod communities, currently almost inexistent.

Keywords

Albufera of Valencia, anthropogenic impacts, coastal lagoon, geochemistry, Ostracoda, rice agriculture

Received 8 February 2012; revised manuscript accepted 3 October 2012

Introduction

Coastal lagoons are usually shallow water bodies outflowing to the sea separated from it by a barrier. Depending on the hydrological balance, the chemistry of these systems can vary from freshwater to hyperhaline environments. Coastal wetlands have been subject to human impacts through fishing, aquaculture, agriculture, hydrology management, and tourism and urban development during the last 100 years (Halpern et al., 2008; Lotze et al., 2006). The human influence could affect their ionic composition usually by causing salinity changes of the water through hydrological modifications, e.g. agricultural activities (Hargrave, 1991; Wetzel, 1983). Furthermore, agricultural, industrial and domestic sewage discharges affected their nutrient balance (increasing eutrophication processes) driving the consequent habitat degradation and loss of biodiversity (Halpern et al., 2008; Lotze et al., 2006).

Ostracods (bivalved microcrustaceans) are commonly found in coastal Quaternary sediments and have been widely used in paleoenvironmental reconstruction, particularly as hydrodynamic and salinity indicators in marine/lagoon transitional environments (Anadón et al., 2002; Carbonel and Peypouquet, 1983; Frenzel and Boomer, 2005). Furthermore, lagoonal salinity variations and climatic events such as storms or tsunamis can also be reflected in the ostracod assemblages, modifying species composition (Carbonel and Jouanneau, 1982; Ruiz et al., 2010) and geochemical signals (Anadón et al., 2002; Marco-Barba et al., 2012). Hence, paleolimnological studies using ostracod remains, abundant in coastal wetlands, have helped to understand climatic changes and anthropogenic impacts, even to detect important historical events that remain not clear in documentary archives (Anadón et al., 2002; Boomer and Eisenhauer, 2002; Keatings et al., 2007; Primavera et al., 2011).

The Albufera of Valencia, one of the largest lagoons in the Mediterranean coast of the Iberian Peninsula has experienced important alterations due to changes in the socio-economic structure and land uses in its heavily populated surroundings in historical times, namely a decrease in salinity revealed by diatom, charophyte and mollusc remains (Margalef and Mir, 1973; Robles et al., 1985; Rodrigo et al., 2009; Soria, 2006) and an increase in trophic level (Vicente and Miracle, 1992), although the time frame for the strongest salinity changes is still lacking precision. Data on the ostracod fauna of the lake is scarce, with the exception of the work by Poquet et al. (2008), where living populations were not found on top of sediment samples in Albufera of Valencia, but shell remains indicated a past rich ostracod palaeoassemblage. Our main objective was to reconstruct the recent limnological history of Albufera of Valencia by combining information from ostracod paleoecology, shell morphology and geochemistry, using updated

[1]Universitat de València, Spain

Corresponding author:
J Marco-Barba, Department Microbiologia i Ecologia, Universitat de València, Dr. Moliner, 50, Burjassot, Valencia E-46100, Spain.
Email: javier.marco@uv.es

ostracod calibrated data. By analyzing the changes in ostracod palaeoassemblages through a sediment record we will show how the Albufera of Valencia became progressively more isolated from the sea, how rice field expansion and human hydrological management affected the salinity of the lake, and how later on increased human pollution led to the local extinction of ostracod communities.

Material and methods

Study area

The Albufera of Valencia, located in the Mediterranean coast of the Iberian Peninsula, near the town of Valencia, is a shallow coastal lagoon enclosed in the Albufera Natural Park, mostly dedicated to rice farming. It occupies nowadays an approximate surface area of 21 km^2, with a mean depth of about 1 m, being the remnant of a formerly much larger lagoon basin, now mostly transformed into rice fields. A sand bar separates the lagoon from the Mediterranean Sea. The lake level is currently regulated by sluice gates located in the three outflow canals to the sea, according to the needs for rice culturing. Today, a dense human population and numerous industries surround the Albufera of Valencia. The lake conductivity varies between 1 and 3 mS/cm and it is hypereutrophic (Vicente and Miracle, 1992). The Albufera of Valencia is currently a turbid lake dominated by dense phytoplankton populations, mainly cyanobacteria, and macrophytes are absent (Romo et al., 2005; Vicente and Miracle, 1992). However, recent past conditions were quite different; it is known that the average planktonic chlorophyll was below 20 µg/l in 1972 (Dafauce, 1975) and that the lake was covered by a dense submerged macrophyte meadow in the 1950–1960s (Docavo, 1979).

Core extraction, dating and ostracod analysis

Two 63 cm cores were taken in October 2004 at the west of Albufera Lake (Figure 1) close to 'Mata l'Antina' (UTM: 30S 0726941/4357037), one of the vegetation outgrowths inside the lake. The cores were extracted using a gravity corer (designed to obtain undisturbed cores for ^{210}Pb dating) with 8.6 cm liner inner diameter. Both cores were extruded and sliced every centimeter in the field. Subsamples from one of the cores were used for ostracod analysis and subsamples from the other for radiodating analysis. ^{210}Pb and ^{137}Cs analysis were performed at the Autonomous University of Barcelona (for further details see Miracle et al., 2013).

Ostracods were analyzed at 1 cm intervals. Subsamples of about 10 g were sieved through 400 and 250 µm pore size and processed following the methods described by Griffiths and Holmes (2000). Ostracods valves were counted per sample and the abundance expressed as number of valves per 10 g of dry weight. The different species were identified following Athersuch et al. (1989), Meisch (2000) and Poquet et al. (2008).

Morphological and geochemical analysis of Cyprideis torosa shells

Lengths of female and male *C. torosa* valves were measured, as well as the percentage of noded animals per sample, to be used as indicators of salinity variations (Van Harten, 1975; Vesper, 1972a, 1972b).

Between one and five analyses per sample were made to determine isotopical analyses ^{18}O/^{16}O and ^{13}C/^{12}C and trace elements Ca, Mg and Sr from ostracod valves. For each analysis, two or three adult valves or four or five juvenile valves belonging to A-1 and A-2 (and in a few cases A-3) instars were pooled together. Ostracod valves were selected only if belonging to a transparent preservation class as defined in Griffiths and Holmes (2000) and cleaned using the method described in Ito (2001). The samples were analyzed using a Kiel-II online carbonate preparation device coupled to a Finnigan MAT 252 stable isotope ratio mass spectrometer at the University of Minnesota and the residue of this analysis was used for trace elements.

Numerical analyses

We calculated the Shannon-Wiener diversity index (Shannon and Weaver, 1963) as diversity and Evenness (E) to know how the species were distributed per sample (Margalef, 1974). These are among the most common diversity indices used in ecology and therefore can be easily compared with many previous works. In addition, we used the index of fluctuations D_0 formulated by Dubois (1973) as Taylor's expansion of the diversity index H to assess ostracod community fluctuations with respect to the average state calculated for the whole sequence.

$$D_0 = \sum_{i=1}^{S} p_i \log_2(p_i / \overline{p}_i) \quad (1)$$

Where $\overline{p}$ =mean p_i. D_0 is a function of time representing the deviation of the species proportions through time from an average state.

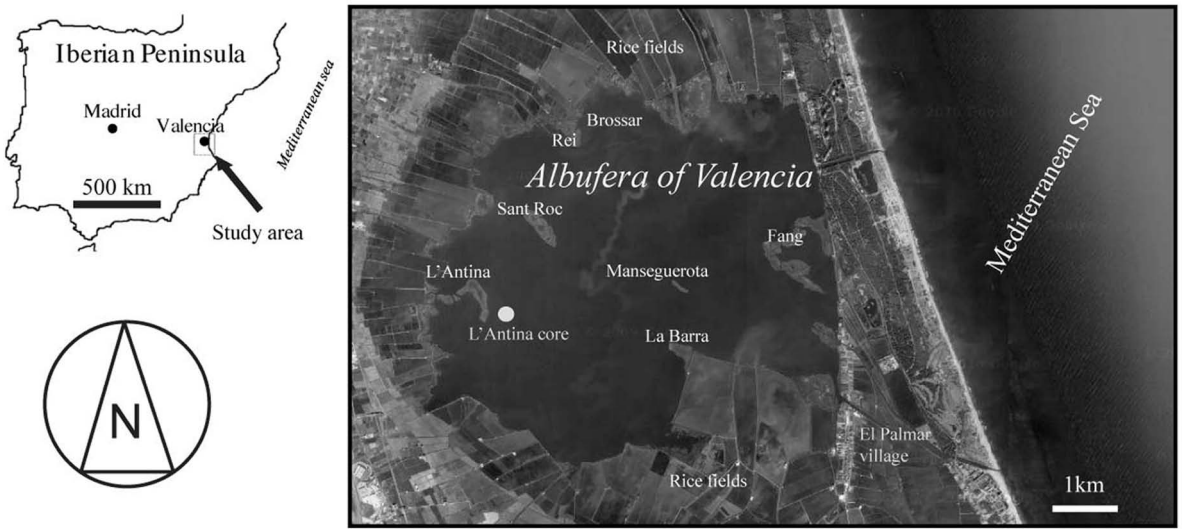

Figure 1. Location of lake 'Albufera de Valencia' in the Iberian Peninsula (left) and aerial picture of the lake (right), showing core 'L'Antina' site.

High values indicate major fluctuations of the community and maximum deviations from the state to which the structure of the community is approaching (Mezquita and Miracle, 1997; Miracle, 1978).

Biostratigraphical zones were obtained by a constrained cluster analysis applying the CONISS method and the Edwards and Cavalli-Sforza distance (Grimm, 1993) to the data matrix of log transformed numbers of valves per 10 g of dry weight of each ostracod species in each core sample. The same matrix was analyzed by means of Principal Component Analysis (PCA) (using the MVSP software) in order to obtain an ordination of samples for a further evaluation of ecological similarities among them. In addition, we used an unconstrained cluster analysis (UPGMA similarity algorithm and the Bray-Curtis distance) to determine ostracod species assemblages and sample groups according to their ostracod community composition. Two samples with no ostracod remains were excluded from the analysis (6.5 cm and 17.5 cm core depth).

The equation obtained in a previous calibration study (Marco-Barba et al., 2012), based on *C. torosa* geochemistry, was used to reconstruct lagoon water changes in past total Sr/Ca ratio:

$$(Sr/Ca)_{WATER} = 1.78 + [1.636*(Sr/Ca)_{VALVE}] \quad (2)$$

Paleosalinity reconstruction of lake Albufera from Antina Core was carried out using ostracod-based weighed averaging transfer functions (TF). Most of the species' optima and tolerances used for this reconstruction were obtained from a published conductivity TF for the Iberian Peninsula by Mezquita et al. (2005). In the case of *Candona angulata* (GW Müller, 1900) and *Bradleystrandesia* cf. *reticulata* (Zaddach, 1844), which were not included in the mentioned training set, we used the conductivity TF from Reed et al. (2012). In the case of *Leptocythere* cf. *porcellanea* (Brady and Robertson, 1869) (without published TF information) we calculated the salinity optimum and tolerance values by weighted averaging the raw data reported by Ruiz et al. (2000b) for the southern Iberian Peninsula. Only for *Cyprideis torosa* we adjusted its influence on the TF by applying a correction factor of 0.1 to core valve densities, in order to give less weight to this species on the salinity reconstruction, as it has a wide tolerance to salinity, and a much stronger (thus durable) shell than other species.

Results

Core description and chronology

Four sedimentary facies were clearly distinguished: facies A, B, C and D (Figure 2). Facies A formed by olive gray-colored sandy silt sediments with abundant bioclasts of mollusks, mainly *Cerastoderma glaucum* (Poiret, 1789) valves, and foraminifers. Facies B formed by very fine homogeneous silt with gray coloration. Bioclasts of molluscs or articulated valves were scarce or absent. Facies C was made up by ochre silt sediments with a small proportion of sand and highly enriched in plant remains. Facies D from 27 cm to the top was formed by homogeneous silt (including two narrow layers with a small proportion of fine sand at the top). The layer shows very few plant and almost no mollusk remains.

We inferred the chronology indicated on Figure 2 from the model of Miracle et al. (2013) based on ^{137}Cs and ^{210}Pb profiles. In summary, the CRS ^{210}Pb model places the year 1963 very close to 30 cm, the depth of a well resolved ^{137}Cs peak that may record the 1963 atmospheric fallout maximum. The dating of the base of the core was fitted with historical data assuming that facies B of fine silt corresponds to a period of very poor drainage of the lagoon during the XIX century, that ended with the opening of a new outflow canal to the sea in 1876, named today Gola del Perellonet.

Ostracod abundances, cluster analysis and PCA

Approximately 15,000 ostracod valves, representing 18 species from 17 genera of ostracods were identified (Figure 3). Three of these taxa were only identified to genus level, mainly because of the low number of valves.

Application of stratigraphically constrained cluster analysis (Figure 3) allowed the differentiation of three main stratigraphical

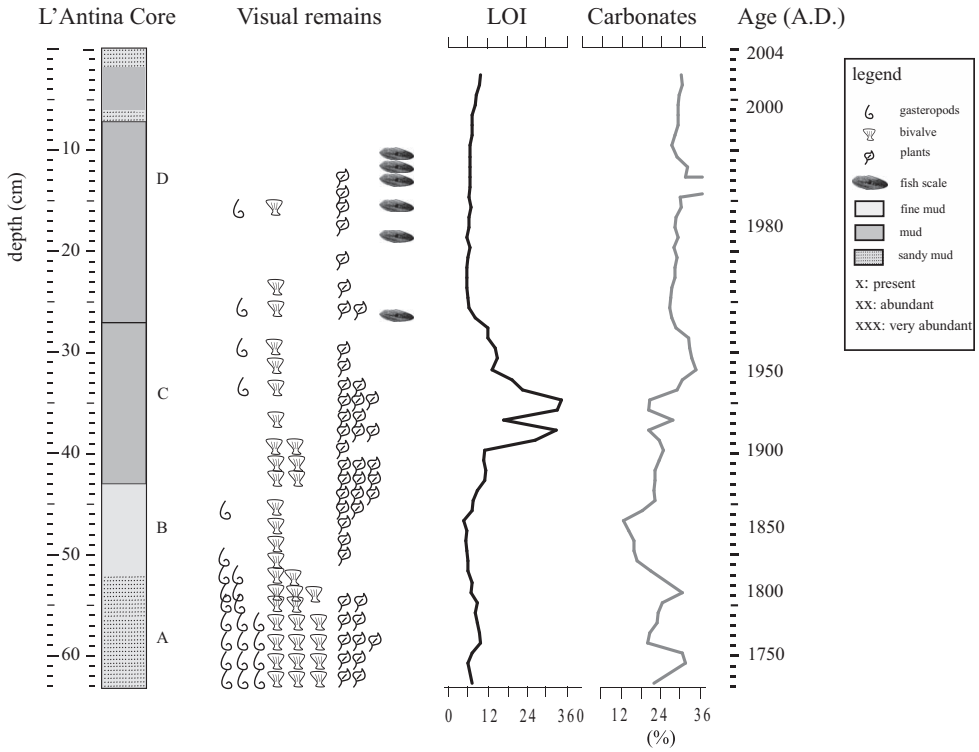

Figure 2. Lithological facies, visual remains, LOI, % carbonates and chronology based on ^{137}Cs and ^{210}Pb of L'Antina Core.

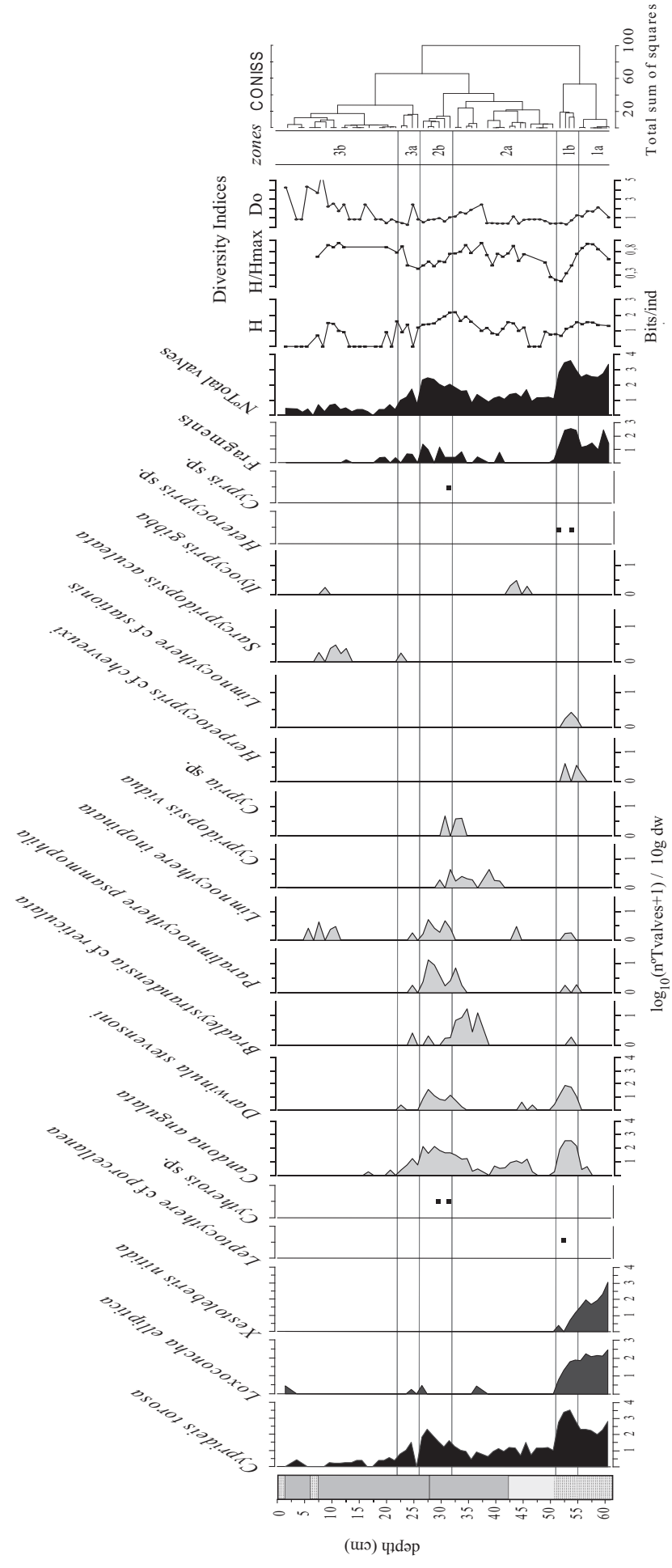

Figure 3. Ostracod abundances and diversity indices in core L'Antina. The total numbers of valves as well as the number of valve fragments are also indicated. Abundances are expressed in valves per 10 g dry weight in $\log_{10}$ scale. Dots indicate species presence. Shannon diversity (H), Evenness (H/H_{MAX}) and Dubois fluctuation index (D_0) are also shown. Zones established by the constrained cluster analysis (CONISS) are indicated at right. Different species colors indicate: euryhaline (*C. torosa*; black), brackish (dark gray) and freshwater (light gray).

zones, which could be further subdivided onto six different subzones. The first zone (zone 1) covers from 63 to 52 cm depth. This zone presented the highest ostracod abundances along the core and corresponds to facies A. It could be further subdivided into two subzones: 1a and 1b. Subzone 1a (from 63 to 55 cm) is dominated by the euryhaline *Cyprideis torosa* and the brackish species *Loxoconcha elliptica* (Brady, 1868) and *Xestoleberis nitida* (Liljeborg, 1853). The very high abundances of ostracod remains (Figure 3) found at the bottom of this subzone are remarkable, especially for *X. nitida*. However, the abundances of these brackish species decrease to the top of this subzone, where *Candona angulata* and *Herpetocypris chevreuxi* (GO Sars, 1896) appear although with very low abundances. Subzone 1b corresponds to a narrow layer from 55 to 52 cm depth of great faunal change. At this point, the abundance of *L. elliptica* and *X. nitida* decreases drastically and these species practically disappear from the sedimentary sequence above this zone. On the other hand, *C. torosa* has a peak of abundance. However, this subzone is characterized by high abundances of the freshwater species *C. angulata* and *Darwinula stevensoni* (Brady and Robertson, 1870). Moreover, it is also remarkable the appearance of other minority freshwater species (*Bradleystrandesia* cf. *reticulata, Paralimnocythere psammophila* (Flössner, 1965), *Limnocythere inopinata* (Baird, 1843), *Limnocythere* cf *stationis* (Vavra, 1891), *Heterocypris* sp., *Cypris* sp.).

Zone 2 covers from 51 to 26 cm depth and could be further subdivided into two subzones: 2a and 2b. This zone corresponds mainly to facies B and C. Subzone 2a is the longest, covering 51 to 32 cm. The number of ostracod valves is much lower than in Zone 1. *Cyprideis torosa* and *C. angulata* showed similar abundances. It should be noticed the significant occurrence of *D. stevensoni, Limnocythere inopinata* (Baird, 1843) and *Ilyocypris gibba* (Ramdohr, 1808) at the lower half of this subzone. At its top half, we observed a shortfall (at 38.5 cm), followed by a recovery of *C. angulata* abundances plus the appearance and increase of the freshwater species *Cypridopsis vidua* (OF Müller, 1776) and *Bradleystrandesia* cf. *reticulata*, with their occurrence practically restricted to this part of the profile. At subzone 2b (from 32 to 27 cm), the total number of valves increased, being the most abundant species *C. torosa, C. angulata* and *D. stevensoni*, with a noteworthy appearance of *P. psammophila* and *L. inopinata*, characteristic of this subzone.

Zone 3 corresponds to facies D. It was subdivided into two subzones. Subzone 3a from 26 to 22 cm is a transition zone with low abundances of *C. torosa* and *C. angulata* accompanied by a few valves of *Bradleystrandesia* cf. *reticulata, P. psammophila* and *L. inopinata* at the bottom half of this subzone and a few valves of *Sarscypridopsis aculeata* (Costa, 1847) at its top part. The last subzone (3b) from 22 to 0 cm presented extremely low abundances of ostracod valves and fragments. However, a few individuals of *C. torosa* are still present in most samples and minoritary species, such as *S. aculeata* and *L. inopinata*, can also be found at the mid part of this subzone.

The PCA results are shown in Figure 4. The main factor (F1) accounted for 57.9% of the total variance and the second (F2) for 30.3%. The species with higher weights on Axis 1 were *C. torosa, L. elliptica* and *X. nitida* on the positive part and *S. aculeata I. gibba* and *C. vidua* on the negative one. *Xestoleberis nitida* and *L. elliptica* were the species with highest positive loads on Axis 2 and *C. angulata* and *D. stevensoni* presented the highest loads on the negative part (Figure 4). Samples and species were ordered on the PCA graph in accordance to the groups obtained with the cluster analyses.

The unconstrained cluster analysis of ostracod species resulted in three main groups (A, B and C). Group A included the most abundant freshwater species. Group B included the less abundant freshwater species (Figure 4), together with brackish species *Leptocythere* cf. *porcellanea* (Brady and Robertson, 1869) and *Cytherois* sp. which were probably included in this group because of their low abundances, suggesting that this material was reworked from other

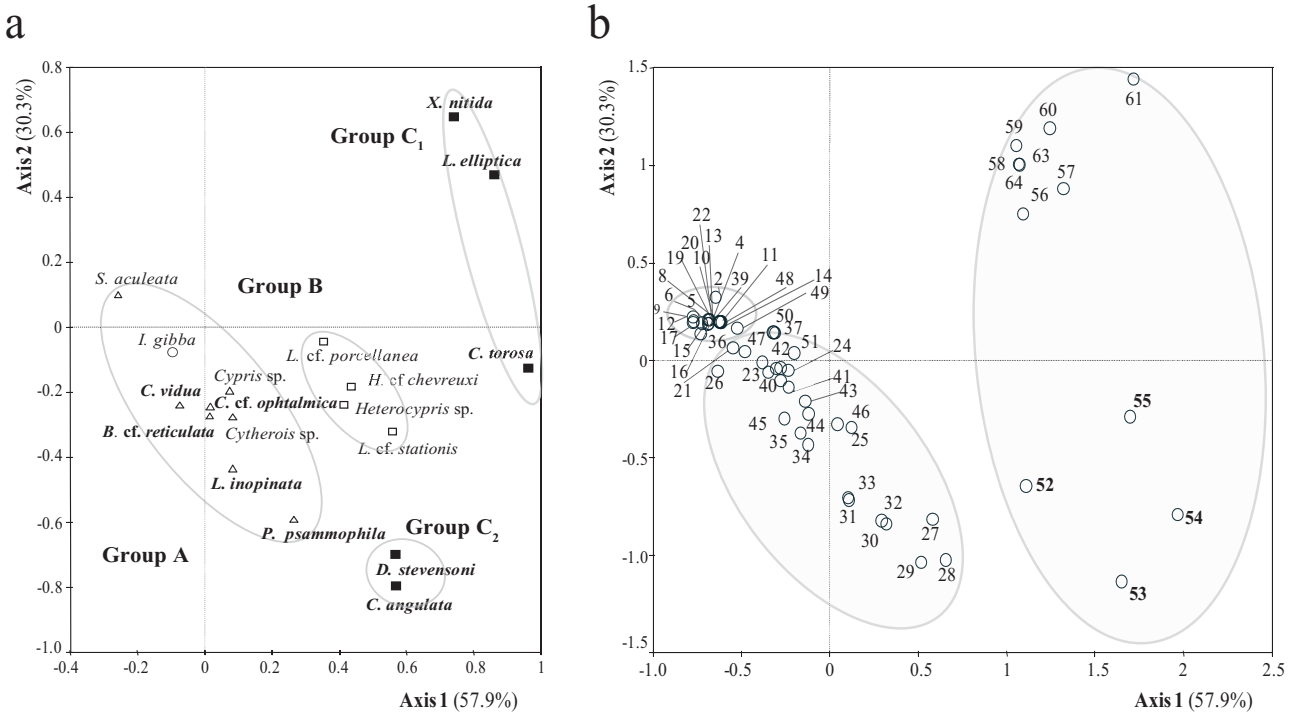

Figure 4. Principal components analysis (PCA) ordination graphs (two first factors) of ostracod species and samples for L'Antina core. (a) Ostracod species ordination diagram. The main groups of species obtained by unconstrained cluster analysis are indicated with ellipses and different symbols: Group A: open triangles; Group B: open squares; Group C: solid squares (subgroups C_1 and C_2 are also placed). Open circles correspond to the less common species (*I. gibba*). The most abundant species (>10 valves) are marked in bold type. (b) Samples ordination graph. Sample labels correspond to core depth and are delimited by ellipses corresponding to groups obtained from the unconstrained cluster analysis.

parts of the lake. Group C included the euryhaline species *C. torosa* and the brackish and phytophilous species *L. elliptica* and *X. nitida* (Subgroup C1) and the freshwater, but halotolerant species, *D. stevensoni* and *C. angulata* (Subgroup C2).

Diversity indices

Regarding ostracod diversity indices (Figure 3), the minimum values corresponded to subzone 3b (with a very scarce, poor ostracod fauna) and a few other individual samples related to changing conditions (e.g. between zones 1–2 and 2–3). Shannon diversity (*H*) showed the highest values at subzone 1a and at the upper part of subzone 2a (1.6–2.2 bits/ind.). Diversity indices remained high at subzone 1a, and decreased at subzone 1b. At subzone 2a abrupt diversity changes were registered but in general it showed a tendency to increase with decreasing depth, until subzone 2 where it decreased constantly. Subzone 3a seems to be a period of changing conditions, where abrupt changes in diversity indices were registered. Subzone 3b showed the lowest diversity indices but with sudden upsurges that should be taken with caution because of the low number of valves found.

Zones with values of the fluctuation index D_0 close to zero (1b, mid and bottom parts of 2a, 2b and 3a) indicated periods closest to the average community (dominated by *C. torosa*). In contrast, subzone 1a showed higher D_0 values indicating large differences in ostracod assemblages with respect to the average state. But also subzone 3b and singular samples at other subzones had maxima of this index; in this case, these high values are indicating perturbations, which are also associated with low values of diversity indices.

Cyprideis torosa ecophenotypic responses

Cyprideis torosa carapace length of a total of 753 individuals were measured in the 22 core samples where adults were present; 371 were females and 382 males (Figure 5; Table 1). LOESS regression was applied for females and males separately and both followed the same trend at all biostratigraphic zones. Valve length was significantly correlated with the following shell chemistry variables: positively with Ca (*r*: 0.35; $p<0.05$) and Sr/Ca (*r*: 0.53; $p<0.01$) and negatively with $\delta^{18}O_{VPDB}$ (*r*:−0.41; $p<0.01$).

All the counted valves were checked for the presence of nodes (Figure 5; Table 1). The valves found at the bottom of the core, subzone 1a, were smooth and the percentage of noded forms increased slightly to the top of this subzone. Subzone 1b showed small peaks in percentage of noded valves at its bottom and top. Subzone 2a showed alternating layers of noded and smooth forms reaching the highest percentages of noded valves at the bottom half of this subzone. Subzone 2b presented high percentages of noded valves at its bottom half, however, the percentages were lower at its top. Subzone 3a showed a small peak at the bottom. Finally, in subzone 3b, owing to the very low number of *C. torosa* valves which may probably consist of reworked remains, only very few noded individuals were found (see Table 1; percentages per sample could not be calculated because of insufficient number of individuals)

Element ratios in *C. torosa* calcite

Mg/Ca molar ratios in *C. torosa* valves are plotted in Figure 5 and the average values for each sample can be seen in Table 1. Mg/Ca ranged from 5.9×10^{-3} to 21.9×10^{-3} (average value of 11.4×10^{-3}) along the core, with highest average values at subzone 2a. This range of values is similar to that obtained for current *C. torosa* populations from Spanish Mediterranean wetlands with water molar Mg/Ca<6 (Marco-Barba et al., 2012).

Sr/Ca ranged from 3.63×10^{-3} to 9.58×10^{-3} (average value of 6.47×10^{-3}) along the core (Figure 5; Table 1). At the bottom of the core Sr/Ca was low (5.1×10^{-3}) and showed low variability but it presented a clear increasing trend upwards until zone 2, reaching an average value of 6.9×10^{-3}, though variability was very high at subzone 1b. At subzone 2a this ratio maintained high values (average of 7.6×10^{-3}) and had low variability. At subzones 2b and 3a the ratio was relatively constant with an average value of 6.53×10^{-3} and low variability. Only one analysis was carried out at subzone 3b; where Sr/Ca presented a relatively high value (7.65×10^{-3}).

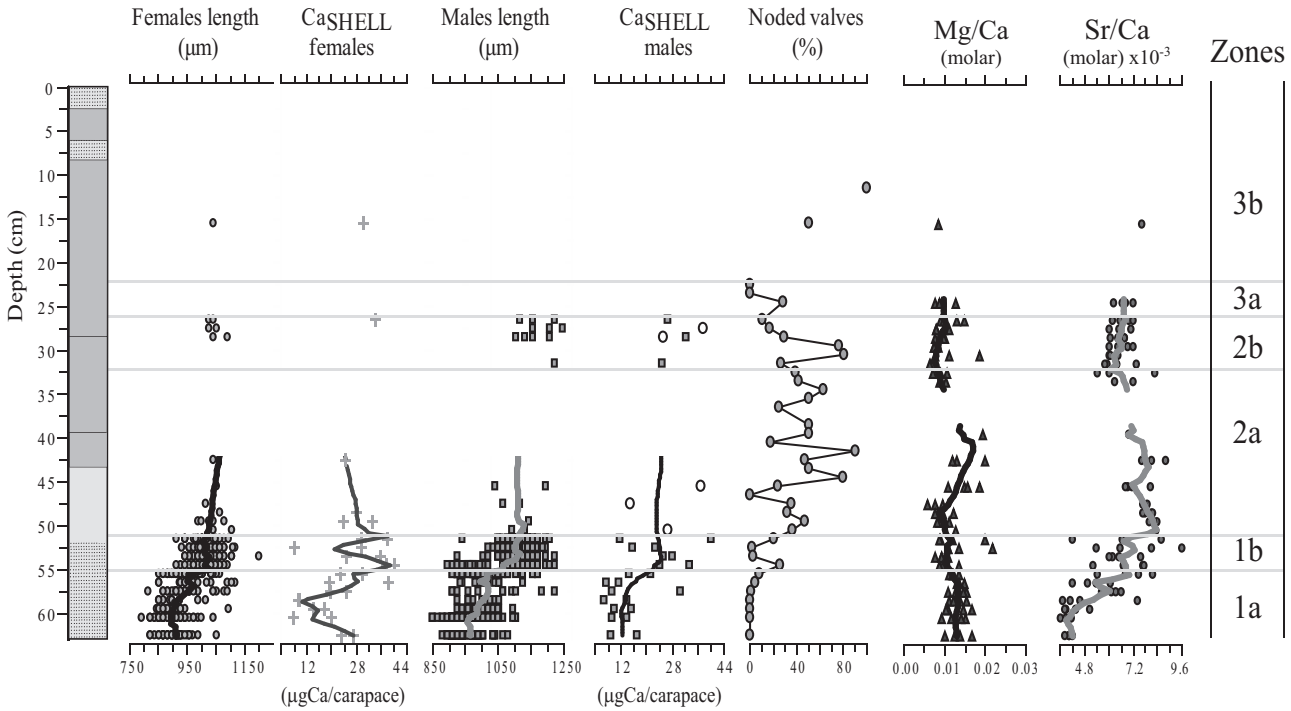

Figure 5. Profiles of morphological and geochemical variables of *Cyprideis torosa* shells: female and male shell length and Ca content (Ca_{SHELL}) per valve; percentage of noded valves, shell Mg/Ca and Sr/Ca molar ratios. Loess regressions were performed for most of the variables shown. Note: white circles in Ca_{SHELL} values indicate samples where males and females were mixed together in the analysis.

Table 1. Morphological and geochemical information of *Cyprideis torosa* remains: total number of valves per 10 g of dry weight, number of valves of each sex and age (adults, adult females, adult males and juveniles), number of noded valves, number of black (preservation state) valves, valve length for females and males (including mean ± SD and measured valves for each case), Mg/Ca and Sr/Ca molar ratios and isotopical variables ($\delta_{13CVPDB}$ and $\delta_{18OVPDB}$) (including mean ± SD and the number of analyses done).

Depth (cm)	Total number of valves ($10gdw^{-1}$)	Adults	Females	Males	Juveniles	No. noded valves	black	Females length (μm)	Valves measured	Males length (μm)	Valves measured	Mg/Ca (molar) $\times10^{-3}$ SD	Sr/Ca (molar) $\times10^{-3}$ SD	$\delta^{13}C_{VPD\ B}$ (‰) SD	$\delta^{18}O_{V\ P\ D\ B}$ (‰) SD	Number analyses
2		0														
4	2	0			2											
5	1	0			1											
6		0														
7		0														
8		0														
9		0														
10	1	0			1											
11	1	0			1											
12	1	0			1	1										
13	1	0			1											
14	1	0			1											
15	2	0			2											
16	2	1	1		1	1		1040	1			8.59	7.65	–0.14	–1.35	1
17		0			0											
18		0			0											
19	2	0			2											
20	2	0			2											
21	4	0			4											
22	2	0			2											
23	7	0			7											
24	13	0			13											
25	39	1	1		38	11						9.58 ± *2.13*	6.74 ± *0.39*	–5.58 ± *0.86*	–2.31 ± *0.15*	4
26		0			0											
27	96	5	2	3	91	10		1033.5 ± *9.2*	2	1165.7 ± *52.5*	3	11.64 ± *2.77*	6.75 ± *0.47*	–4.75 ± *0.98*	–2.56 ± *0.79*	4
28	205	5	2	3	200	34		1040 ± *18.4*	2	1204.7 ± *45.7*	3	9.17 ± *1.56*	6.55 ± *0.43*	–4.27 ± *1.15*	–2.49 ± *0.60*	4
29	97	6	2	4	91	28		1066 ± *36.8*	2	1150.5 ± *44.4*	4	9.13 ± *0.99*	6.53 ± *0.34*	–3.85 ± *0.79*	–2.69 ± *0.55*	4
30	38	0			38	29						7.82 ± *0.55*	6.66 ± *0.52*	–5.10 ± *0.70*	–2.41 ± *0.42*	4
31	21	0			21	17						12.48 ± *5.49*	6.20 ± *0.23*	–4.27 ± *1.22*	–2.77 ± *0.13*	3
32	52	2		2	50	14				1222.0	1	6.90 ± *0.45*	6.39 ± *0.71*	–6.27 ± *1.96*	–2.50 ± *0.72*	4
33	23	0			23	9						8.88 ± *1.72*	6.60 ± *1.48*	–7.04 ± *0.40*	–2.39 ± *0.47*	2
34	12	0			12	5						9.52 ± *1.07*	6.76 ± *0.67*	–9.05 ± *0.24*	–2.21 ± *0.16*	2
35	8	0			8	5										
36	2	0			2	1										
37	8	0			8	2										
38		0			0											
39	2	0			2	1										

(Continued)

Table 1. (Continued)

Depth (cm)	Total number of valves ($10gdw^{-1}$)	Adults	Females	Males	Juveniles	No. noded valves	black	Females length (μm)	Valves measured	Males length (μm)	Valves measured	Mg/Ca (molar) $\times 10^{-3}$ SD	Sr/Ca (molar) $\times 10^{-3}$ SD	$\delta^{13}C_{VPD\ B}$ (‰) SD	$\delta^{18}O_{VPDB}$ (‰) SD	Number analyses
40	10	0			10	5						19.4 ± *19.43*	*7.0 ± 7*	–6.9 ± *–6.87*	*–1.1 ± –1*	1
41	17	0			17	3										
42	10	0			10	9										
43	15	2	2		13	7		1040	1			15 ± *4.31*	*8.2 ± 1*	–4 ± *6.31*	*–0.2 ± 2.5*	2
44	14	0			14	7										
45	5	0			5	4										
46	37	4	2	2	33	9		1053	1	1118 ± *110.3*	2	15 ± *3.20*	*7.2 ± 0.6*	–5 ± *0.16*	*–1.2 ± 0.7*	4
47	6	0			6											
48	17	3	1	2	14	6		1014	1	1092 ± *36.8*	2	7.8 ± *1.87*	*7.8 ± 0.1*	–4.6 ± *0.19*	*–1.6 ± 0.3*	3
49	19	2	2	0	17	6		1066	1			9.5 ± *2.03*	*7.9 ± 0.2*	–4.5 ± *0.68*	*–1.5 ± 0.7*	4
50	17	8	6	2	9	8		1027 ± *35.6*	5	1144	1	9.6 ± *1.34*	*8.2 ± 0.2*	–4.2 ± *0.51*	*–0.9 ± 0.7*	4
51	11	4	2	2	7	4		1072.5 ± *46.0*	2	1111.5 ± *27.6*	2	212.6 ± *12.63*	*8.3 ± 8.3*	–3.7 ± *–3.74*	*–0.3 ± –0*	1
52	749	65	29	36	684	152	43	1008.1 ± *45.2*	25	1116.2 ± *53.4*	31	12.4 ± *5.25*	*6.6 ± 1.8*	–3.6 ± *0.73*	*–1.1 ± 2.1*	4
53	3323	240	115	125	3083	71	94	1015.2 ± *40.7*	44	1100.0 ± *43.9*	45	14.3 ± *5.18*	*7.4 ± 1.8*	–1.9 ± *3.08*	*–0.3 ± 0.6*	4
54	4078	375	128	247	3703	121	346	1020.2 ± *54.2*	36	1103.9 ± *55.5*	37	9.4 ± *1.31*	*6.6 ± 0.7*	–2.5 ± *1.14*	*0.5 ± 1.3*	4
55	935	300	93	207	635	240	138	1011.3 ± *43.2*	35	1065.3 ± *86.6*	43	10.6 ± *2.07*	*6.8 ± 1.2*	–2.1 ± *0.89*	*–0.4 ± 0.4*	4
56	284	87	46	41	197	22	15	953.9 ± *52.6*	50	1013.9 ± *77.9*	37	12.1 ± *0.98*	*7.0 ± 1.2*	0.2 ± *1.16*	*0.5 ± 1.2*	4
57	256	33	17	16	223	11	3	984.3 ± *87.6*	13	1017.5 ± *52.9*	12	13.7 ± *0.89*	*5.2 ± 0.8*	–3.9 ± *1.99*	*1.0 ± 0.7*	4
58	232	39	28	11	193	3	0	946.7 ± *66.9*	28	1039.2 ± *108.1*	11	13.4 ± *2.04*	*6.2 ± 0.4*	–2.6 ± *2.12*	*2.1 ± 0.8*	4
59	114	22	10	12	92	0	0	910.0 ± *54.6*	10	992.0 ± *45.1*	8	13.1 ± *1.89*	*5.0 ± 2*	–5.1 ± *1.51*	*0.5 ± 1*	4
60	214	58	28	30	156	0	1	897.9 ± *49.2*	24	985.5 ± *42.6*	26	13.1 ± *3.09*	*4.3 ± 1*	–6.3 ± *0.34*	*1.0 ± 1*	4
61	832	167	72	95	665	0	0	896.4 ± *51.2*	45	963.7 ± *58.4*	59	13 ± *2.70*	*4.0 ± 0.2*	–6.1 ± *1.20*	*2.1 ± 1*	4
63	368	102	45	57	266	0	0	908.7 ± *44.0*	43	959.1 ± *45.1*	55	13.3 ± *2.85*	*4.1 ± 0*	–6.2 ± *1.49*	*1.4 ± 1*	4

Isotope results

Isotopic results for *C. torosa* shells are shown in Figure 7, and average values for each sample can be seen in Table 1. $\delta^{13}C_{VPDB}$ ranged between −9.22‰ and 2.95‰ (mean value −4.35‰) along the core and $\delta^{18}O_{VPDB}$ ranged between −3.49‰ and 3.73‰ (mean value of −1.78‰) along the core.

$\delta^{13}C_{VPDB}$ showed low values at the bottom of subzone 1a but higher variability and higher values towards the top of it (mean: −4.29±2.65), reaching the highest values of the entire sequence. $\delta^{13}C_{VPDB}$ was correlated with shell Ca content (r: 0.607; $p<0.01$) and with Sr/Ca (r: 0.706; $p<0.01$) in this subzone. However in subzone 1b, $\delta^{13}C_{VPDB}$ followed a decreasing trend upwards through this and the next subzone (1b and 2a) with a much lower variability. $\delta^{13}C_{VPDB}$ was negatively correlated with Sr/Ca (r: −0.546; $p<0.05$) in subzone 1b. On the other hand, $\delta^{18}O_{VPDB}$ showed the highest values of the entire core at its bottom (mean: 1.23±1.18) descending towards the top of subzone 1b.

Both, $\delta^{13}C_{VPDB}$ and $\delta^{18}O_{VPDB}$ values in subzone 2a were lower than in the previous zone 1 (Figure 7; Table 1) and followed a decreasing upward trend. At subzone 1b and 2a, $\delta^{13}C_{VPDB}$ and $\delta^{18}O_{VPDB}$ isotopic ratios were positively correlated (r: 0.808; $p<0.01$). At subzone 2b, $\delta^{13}C_{VPDB}$ increased and maintained high values, being on average (mean: −4.76‰) higher than in subzone 2a. $\delta^{18}O_{VPDB}$, however, presented lower mean values than in the previous subzone (mean: −2.57‰).

The few analyses carried out at subzone 3a showed $\delta^{18}O_{VPDB}$ values similar to the previous subzone and $\delta^{13}C_{VPDB}$ slightly reduced. The only analysis performed at subzone 3b showed slightly higher isotopic ratios than those of the previous subzone; as we previously mentioned, *C. torosa* remains in the top of the core are probably re-suspended valves.

In Figure 6 we show the subfossil *C. torosa* shell isotopic results together with isotope data from living equivalents collected in modern freshwater, brackish and hypersaline sites in close coastal wetlands, recorded in Marco-Barba et al. (2012).

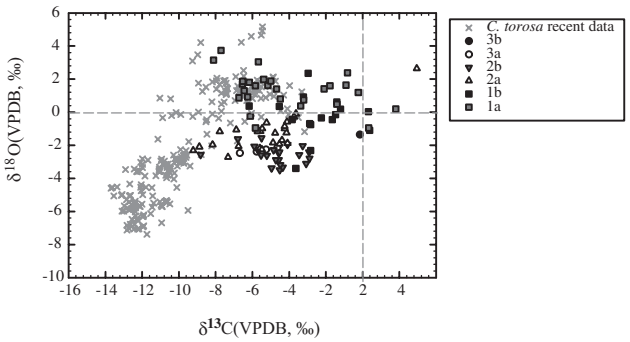

Figure 6. Relationship of stable isotopic composition $\delta^{13}C$ and $\delta^{18}O$ (VPDB notation) of *C. torosa* valves in Core L'Antina and Recent samples from various Spanish Mediterranean coastal wetlands. The established ostracod biozones (1a, 1b, 2a, 2b, 3a, 3b) for core 'L'Antina' are indicated with different symbols. Recent data after Marco-Barba et al. (2012).

The analysed *C. torosa* shells from the lake sediments showed values of $\delta^{18}O_{VPDB}$ within the variability of the shells of present-day ostracod collections. However, $\delta^{13}C_{VPDB}$ values from the Albufera core were in general higher than in other recent sites.

Sr/Ca_{WATER} and salinity reconstructions

Past water Sr/Ca was reconstructed based on Sr/Ca from *C. torosa* shells, and salinity reconstruction was based on ostracod species ecological preferences. The past water chemistry reconstructions are shown in Figure 7. In general, water Sr/Ca was negatively correlated with salinity (r: −0.687; $p<0.01$) although both variables were not correlated for each different subzones separately, probably because of the low range of values within each subzone. The inferred salinity values were the highest and fairly constant through most of zone 1, around 16 g/l on average, but with an

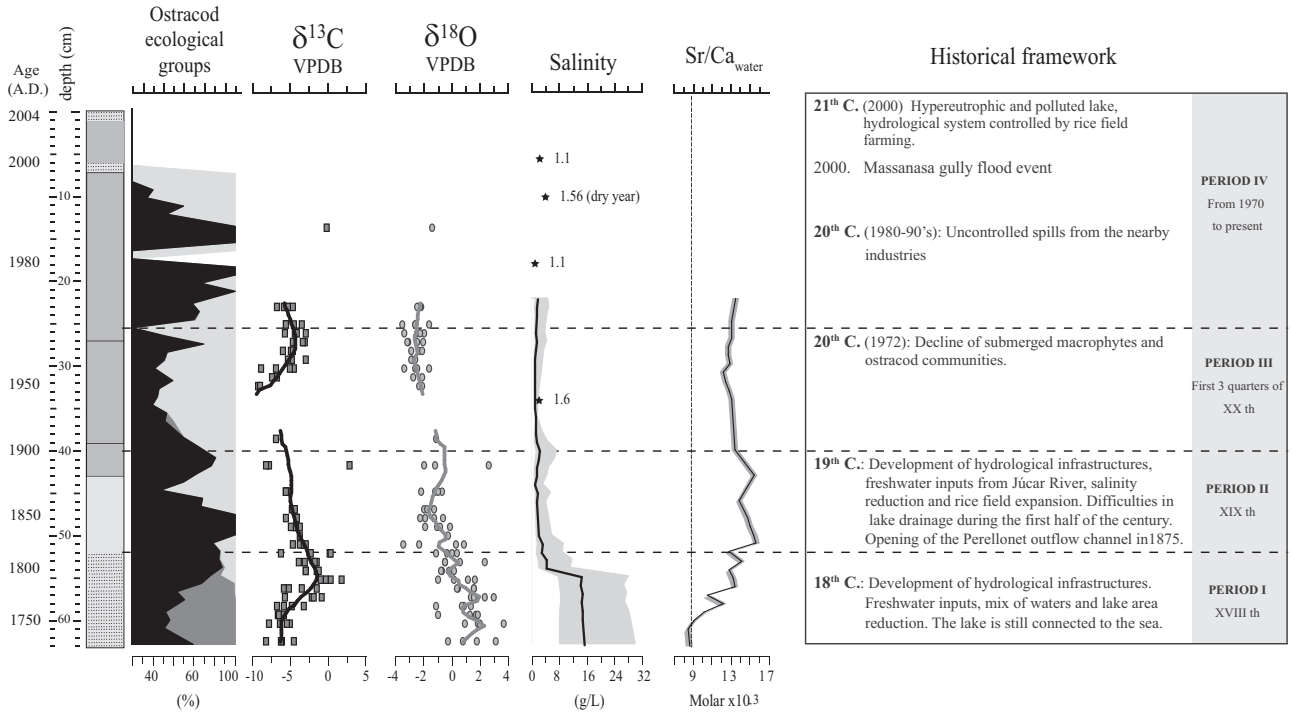

Figure 7. Relative proportions (percentages) of euryhaline (*C. torosa*; black) brackish (dark gray) and freshwater (light gray) ostracod species, together with isotopic ratios ($\delta^{13}C$ and $\delta^{18}O$), transfer function inferred salinity and Sr/Ca_{WATER} and related historical framework. In the inferred water chemistry values, the line indicates the mean estimated value, and shadow areas the minimum and maximum standard errors. Loess regressions were performed for the isotopic ratios. The dotted line indicates the modern Sr/Ca value for Mediterranean seawater. Star symbols indicate instrumental salinity measurements since for the last 70 years, obtained from Serra et al. (1984), Romo et al. (2005) and Soria (2006).

estimated error range between 8 and 28 g/l. However, at the top of this zone inferred salinity suffered a sudden drop to values around 2–12 g/l, and even lower, around 1 g/l or lower on average –close to present day values – through the rest of the sequence. Inferred Sr/Ca of the water, initially estimated at the bottom of the sequence as values of *c*. 0.009, similar to seawater, rise gradually to the top of zone 1 and vary around 0.01 to 0.015 for the rest of the sequence.

Discussion

Comparing the results obtained from the sedimentary record with documented historical events and three decades of limnological studies could be very informative to reconstruct the evolution of Albufera of Valencia during the last two centuries. L'Antina core biostratigraphic zones, based on ostracod assemblages and shell morphology and chemistry, closely match lithological facies, disclosing four main periods in the sedimentary sequence.

Periods 1 and 2, 18th–19th centuries: brackish (mesohaline-polyhaline) lagoon and transitional stage to an oligohaline lagoon

The ostracod paleoassemblages and geochemical analyses along these periods (ostracods zone 1 and part of zone 2; 63–52 and 52–40 cm, respectively) represent a changing environment, varying between an open Albufera influenced by marine water and evaporation processes and therefore with high salinity content (probably mesohaline tending to polyhaline) to an oligohaline lake, with freshwater inputs increasingly derived from irrigation surplus.

The bottom of the core was clearly dominated by a brackish ostracod assemblage; *L. elliptica* and *X. nitida* (salinity range ≈ 8–29 g/l) accompanied by the more euryhaline *C. torosa* (Athersuch et al., 1989; Mezquita et al., 2005). These species are usually found establishing assemblages that tolerate high salinity fluctuations (transitional environments), mainly in estuaries and coastal lakes with muddy sediments enriched in sands (Ruiz et al., 2000a, 2000b, 2006). Diversity indices values indicated rather constant environmental conditions.

The transitional stage to an oligohaline habitat is clearly marked by the decrease of ostracods (particularly *X. nitida* abundances) and the appearance of less halotolerant species such as *C. angulata* or *D. stevensoni* (Meisch, 2000) among others. The presence of a few valves of the brackish *Leptocythere* cf. *porcellanea*, usually found in estuaries and bays (Athersuch et al., 1989) suggests that there is still some seawater interchange and probably they came from outflowing canals. Diversity is here notably reduced at the top of period 1 because of increased dominance of *Cyprideis torosa*, as a result of the changing conditions that favour the growth of this euryhaline species. Furthermore, the increasing freshwater supplies and the increasing agricultural activities favoured, initially, the development of a dense submerged macrophyte meadow that will be later replaced by a phytoplankton dominance with a consecutive macrophyte loss due to increased nutrient input (see below).

The increase of *C. torosa* valve lengths, shell Ca content and the rise of the percentage of noded forms throughout this transitional stage suggest also a reduction in salinity (Marco-Barba, 2010; Van Harten, 1975), owing to increased freshwater inputs and mix of waters. Water Sr/Ca reconstruction (Figure 7) suggests that the bottom of the core was influenced by waters with typical seawater Sr/Ca values (Sr/Ca sea: 8.8×10^{-3} molar ratio; De Villiers, 1999; Renard, 1985; Weinbauer and Velimirov, 1995). However, estimated water Sr/Ca increased to the top of period 1, suggesting the entry of different water sources derived from waters with a higher Sr/Ca ratio. The anomalous high Sr content in the freshwater sources could explain the Sr/Ca increase. This period corresponds with the extension of the main canal derived from Xúquer (=Júcar) river ('Sequia Real del Xúquer') to irrigate rice fields. The increased input into Albufera lagoon of waters derived from Xúquer river (which pass through zones with Keuper geological outcrops) could explain these anomalies, as it has been discussed in relation to results from another core from the same lake (Marco-Barba, 2010) and from other ostracod sequences having similar high Sr anomalies (Anadón and Julià, 1990; Müller, 1968, 1969). In agreement with these data, the high values and the wide scatter of $\delta^{18}O$, and the low $\delta^{13}C$ values at the bottom of the core (Figure 7) suggest brackish waters with a relatively low production/decomposition ratio that are gradually changing to lower salt contents and higher primary production, because of the increasing inflow of nutrient-rich water from irrigated lands. The $\delta^{13}C$ of the DIC in the water is increased by the removal of dissolved inorganic carbon by macrophytes and algae during photosynthesis (fixing preferentially ^{12}C) and by carbonate precipitation (Leng and Marshall, 2004). $\delta^{13}C$ in *C. torosa* valves was correlated with valve Ca and Sr/Ca suggesting a new water source supply. For that reason, we can attribute the increase in $\delta^{13}C$ to the waters with high carbonate contents transported from Xúquer River as a result of increased irrigation, and eventually entering the Albufera system with an additional increase in $\delta^{13}C$ due to higher primary production. On the other hand, $\delta^{13}C$ in the water decreases by the mineralization of ^{13}C depleted organic matter. Then the diminution of $\delta^{13}C$ of *C. torosa* valves at the end of the period 1 (in subzone 1b), after the mentioned relative increase, may be explained by the shift from a brackish water habitat to a oligohaline one, implying the loss and decomposition of brackish macrophytes and the lower production of an incipient new macrophyte community adapted to waters of lower salinity. This is in agreement with a lower inferred salinity, a higher reconstructed Sr/Ca_{WATER} with respect to the bottom of the sequence at this transitional stage (subzone 1b), together with the appearance of freshwater ostracod species.

Ostracod shell $\delta^{18}O$ values in these periods (Figure 7) fall within the range of *C. torosa* populations living today in brackish and hypersaline waters influenced by seawaters in nearby areas. Thus, we suggest that the bottom of the core corresponds to a lagoon influenced by seawater and/or high evaporation processes that increased salinity. There is no correlation between $\delta^{13}C$ and $\delta^{18}O$ values in this period suggesting an open lake, as the $\delta^{13}C$ and $\delta^{18}O$ values for autogenic carbonates in closed-basin lakes often covary (Li and Ku, 1997; Talbot, 1990).

Period 3: first three-quarters of the 20th century

During this period, corresponding to the top of zone 2 (40–26 cm) the Albufera ecosystem was an oligohaline lagoon, as indicated by the low values of the reconstructed salinity with a rich fauna of oligohaline or freshwater ostracods. The euryhaline *Cyprideis torosa* was still one of the most common species, but the increase of *C. angulata, D. stevensoni* and other oligohaline and freshwater species indicate the establishment of freshwater conditions, especially towards the top. In particular, the cosmopolitan freshwater species *Cypridopsis vidua* (salinity range = 0.3–2.3 g/l; Mezquita et al., 2005) and *Bradleystrandesia* cf. *reticulata* and *Cypria* sp. increased also at the top of this zone, indicating a more stable freshwater environment. These species can tolerate a wide type of (freshwater) habitats, temporary or semi-permanent, and they are usually found at high densities in the presence of macrophytes. Indices H and D_0 increased where more freshwater species were found, suggesting changing environments, probably due to increased hydrological instability suggested by the scattered occurrence of different freshwater species (*I. gibba* and *L. inopinata*).

The transitional stage of subzone 2b (Figure 3) is characterized by an increase of the euryhaline *C. torosa* and the diversity index decreased, although freshwater species *P. psammophila* (salinity range = 0.2–1.7 g/l), *L. inopinata* (salinity range = 0.8–3.7 g/l) also occurred together with the most common ones along the core, *C. angulata* and *D. stevensoni*. The scattered presence of brackish species such as *L. elliptica* and *Cytherois* sp. suggest that this material was reworked from other parts of the lake.

C. torosa shell Ca content and valve lengths and the percentage of noded animals indicate also freshwater conditions in this period. Moreover, $\delta^{18}O$ and Sr/Ca remained constant, suggesting freshwater conditions and constant water supply from the same sources. $\delta^{13}C$ showed a slight progressive decline, more pronounced at the beginning of the period. Again, as in period 1, there is a transitional stage (subzone 2b, Figure 5) where changes are made evident by these proxies; Sr/Ca and $\delta^{18}O$ become slightly reduced and $\delta^{13}C$ shows a slight increase. All these data suggest great changes taking place at the second half of the 1960s, with increased industrialization and change of techniques in rice cultivation involving more fertilizers and pesticides (Dafauce, 1975; Soria et al., 1987). Macrophyte cover rapidly reduced (at the end of the 1960s) and was substituted by high phytoplankton biomass and photosynthesis activity (fixing more ^{12}C; Leng and Marshall, 2004).

Period 4 from 1970 to the top

This period corresponds to zone 3 characterized by the abrupt disappearance of ostracod remains. At the transitional stage (subzone 3a), there are still remains of populations of the previously dominant species *C. torosa* and *C. angulata*, but their abundances drastically decreased at the end of this stage. In the top layers of the core (subzone 2b) a few individuals of *C. torosa* and *L. elliptica* were found altogether with freshwater cosmopolitan species *L. inopinata, S. aculeata* and *I. gibba.* These most probably do not accurately represent natural living populations being reworked remains transported from other places (Whatley, 1983). Owing to low abundance of ostracod valves we can only say that most of the few observed individuals of *C. torosa* were noded forms and the few geochemical analyses suggest a freshwater environment (Figure 7) with similar conditions as the previous subzone1b. The ostracod disappearance was probably caused by important changes that occurred in the trophic state of this lake because of increased nutrient input and phytoplankton dominance, which drove the gradual disappearance of its ostracod fauna, a human-induced loss of biodiversity in the lake that was already detected by the study of the current ostracod fauna from surface sediments in this lagoon (Poquet et al., 2008).

Synthesis on the evolution of the Albufera Lake since the 18th century

The study of L'Antina core settled the question on the timing of the main salinity changes. We have shown that the transformation of a brackish to an oligohaline lagoon is much more recent than other authors proposed (Robles et al., 1985; Rodrigo et al., 2009; Sanjaume et al., 1992). Ostracod paleointerpretations clearly indicated a previous brackish stage (before AD 1850) that changed to a freshwater environment to the top of this core (Figure 7). The bottom of L'Antina core is characterized by the typical sediments of a lagoon-barrier system, suggesting that these sediments were influenced by seawater and evaporation processes at that time. High sedimentation rates, inferred Sr/Ca, salinity reduction and ostracod assemblages indicate that the water supply changed from the bottom of the core to the lower half (facies B and C). We hypothesize that this period coincides with the important hydrological control of the lake that took place during the 19th century, intended for the expansion of rice cultivation. Regarding historical archives, important irrigation developments were initiated at the end of the 18th century with the extension of the main canal from Xúquer River ('Acequia Real del Júcar') and the enlargement of the hydrological infrastructure; the main works started in the 1770s, were intensified in 1788–1808 and finished during 1815 (Peris-Albentosa, 1995; Sanchís-Ibor, 2001). This hydrological infrastructure favored the extraordinary rice expansion, through drainage of marshlands and also of the lake littoral; the lake was reduced (5000 ha) between 1865 and 1927. In 1865, Spain was under a notable economic crisis. This crisis and the high economic expenses involved in the management of Albufera were the reasons why Queen Isabel II decided to transfer the property of the lake to the Spanish government (Sanchís-Ibor, 2001), which favored agricultural expansion in the area. Since then, rice farmers control the water supplies for irrigation that eventually flow into Albufera originating from the Xúquer River (with different water Sr/Ca). These water inputs from the irrigation net reduced the salinity of the lake.

Shortly after the salinity reduction and the increased agricultural activities, the Lake Albufera suffered an important eutrophication process that led first to a great macrophyte development and later to a turbid state of phytoplankton dominance and macrophyte loss. Albufera of Valencia became a turbid hypereutrophic lagoon with a dense phytoplankton population, a change that has been documented to occur in the 1970s (Blanco, 1973; Dafauce, 1975; Vicente and Miracle, 1992). The sharp decline in macrophytes abundances also allowed the increase of mugilid fish since the 1950s and the reduction in fish species richness that occurred at Albufera of Valencia especially from 1950 to 2002 (Blanco and Romo, 2006; Docavo, 1979). Since the 1950s mullet (*Mugil cephalus* and *Liza aurata*) captures increased in detriment of predaceous species such as the eel (*Anguilla anguilla*) or *Dicentrarchus labrax* (Blanco et al., 2003). The drastic reduction of macrophyte coverage, the increasing benthic disturbance by wind and fishes, together with anoxia at the bottom substrate, reduced the quality of the benthic environment, being the main reasons for the drastic reduction of the associated fauna (including e.g. ostracods and gastropods).

Funding

The Spanish Ministry of Education and Science (MEC) has funded this research through the project VARECOMED (REN2002-03272). J Marco-Barba acknowledges the funding from MEC, which made possible this work by providing a fellowship (BES-2003-2759) as part of the VARECOMED project.

Acknowledgements

We would like to thank specially Eduardo Vicente Pedrós, who collaborated actively in all the stages of this project and Carlos Santisteban for the sedimentology description. We are also grateful to the University of Minnesota Stable Isotope Lab (Maniko Solheid, manager) for help with the chemical analyses.

References

Anadón BP and Julià R (1990) Hydrochemistry from Sr and Mg contents of ostracodes in Pleistocene lacustrine deposits, Baza Basin (SE Spain). *Hydrobiologia* 197: 291–303.

Anadón P, Gliozzi E and Mazzini I (2002) Paleoenvironmental reconstruction of marginal marine environments from combined paleoecological and geochemical analyses on ostracods. In: Holmes JA and Chivas AR (eds) The Ostracoda: Applications in Quaternary Research. *Geophysical Monograph* 131: 227–247.

Athersuch J, Horne DJ and Whittaker JE (1989) *Marine and Brackish Water Ostracods*. London: Brill EJ.

Blanco C (1973) *Estudio de los rotíferos de la Albufera de Valencia. Influencia de la contaminación en su distribución*. PhD Thesis, University of Madrid.
Blanco S and Romo S (2006) Ictiofauna de la Albufera de Valencia: evolución histórica y situación actual. *Boletín de la Real sociedad española de Historia Natural. Sección Biología* 101(1–4): 45–56.
Blanco S, Romo S, Villena MJ et al. (2003) Fish communities and food web interactions in six shallow Mediterranean lakes. *Hydrobiologia* 506/509: 473–480.
Boomer I and Eisenhauer G (2002) Ostracod faunas as paleoenvironmental indicators in marginal marine environments. In: Holmes JA and Chivas AR (eds) *The Ostracoda, Applications in Quaternary Research*. Washington DC: American Geophysical Union, pp. 135–149.
Carbonel P and Jouanneau JM (1982) The evolution of a coastal lagoon system: Hydrodynamics determined by ostracofauna and sediments. The Bonne-Anse Bay (Pointe de la Coubre). *Geomarine Letters* 1(2): 24–32.
Carbonel P and Peypouquet JP (1983) Ostracoda as indicators of ionic concentrations and dynamic variations: Methodology (Lake Bogoria, Kenya). In: Maddocks RF (ed.) *Applications of Ostracoda*. Houston: Department of Geosciences of the University of Houston, pp. 264–276.
Dafauce C (1975) La Albufera de Valencia. Un estudio piloto. Monografías del Instituto para la Conservación de la Naturaleza. *ICONA* 4: 1–127.
De Villiers S (1999) Seawater strontium and Sr/Ca variability in the Atlantic and Pacific oceans. *Earth and Planetary Science Letters* 171: 623–634.
Docavo I (1979) *La albufera de Valencia. Sus peces y sus aves*. Valencia: Institución Alfonso el Magnánimo.
Dubois DM (1973) An index of fluctuations, D_0, connected with diversity and stability of ecosystems: Applications in the Lotka-Volterra model and in an experimental distribution of species. *Rapport de synthèse III, Programme National sur l'environment Physique et Biologique*. Liège: Project Mer. Commision Interministérille de la Politique Scientifique.
Frenzel P and Boomer I (2005) The use of ostracods from marginal-marine, brackish waters as bioindicators of environmental change and Quaternary palaeoenvironmental analysis – a review. *Palaeogeography, Palaeoclimatology, Palaeoecology* 225: 68–92.
Griffiths HI and Holmes JA (2000) *Non-marine Ostracods and Quaternary Paleoenvironments*. Technical Guide No. 8. London: Quaternary Research Association.
Grimm EC (1993) *TILIA Diagramming Program*. Springfield: Illionis Sate Museum.
Halpern BS, Walbridge S, Selkoe KA et al. (2008) A global map of human impact on marine ecosystems. *Science* 319: 948–952.
Hargrave BT (1991) Impact of man's activities on aquatic systems. In: Barnes RSK and Mann KH (eds) *Fundamentals of Aquatic Ecology*. Oxford: Blackwell Science, pp. 245–264.
Ito E (2001) Application of stable isotope techniques to inorganic and biogenic carbonates. In: Last WM and Smol JP (eds) *Tracking Environmental Change Using Lake Sediments, Vol. 2. Physical and Chemical Techniques*. Kluwer Academic Publishers, pp. 351–371.
Keatings KW, Hawkes W, Holmes JA et al. (2007) Evaluation of ostracod-based palaeoenvironmental reconstruction with instrumental data from the arid Faiyum Depression, Egypt. *Journal of Paleolimnology* 38: 261–283.
Leng MJ and Marshall JD (2004) Palaeoclimate interpretation of stable isotope data from lake sediment archives. *Quaternary Science Reviews* 23(7–8): 811–831.
Li HC and Ku TL (1997) $\delta^{13}C$–$\delta^{18}O$ covariance as a paleohydrological indicator for closed-basin lakes. *Palaeogeography, Palaeoclimatology, Palaeoecology* 133: 69–80.
Lotze HK, Lenihan HS, Bourque BJ et al. (2006) Depletion, degradation and recovery potential of estuaries and coastal seas. *Science* 312: 1806–1809.
Marco-Barba J (2010) *Freshwater ostracods ecology and geochemistry as paleoenvironmental indicators in marginal marine ecosystems: A case of study the Albufera of Valencia*. PhD Thesis, University of Valencia.
Marco-Barba J, Ito E, Carbonell E et al. (2012) Empirical shell chemistry calibration of *Cyprideis torosa* (Jones, 1850) (Crustacea: Ostracoda). *Geochimica et Cosmochimica Acta* 93: 143–163.
Margalef R (1974) *Ecología*. Barcelona: Omega.
Margalef R and Mir M (1973) Indicadors de canvis de salinitat en els sediments de l'Albufera de València. *Treballs Societat Catalana Biologia* 32: 111–117.
Meisch C (2000) *Freshwater Ostracoda of the Western and Central Europe*. (Süβwasserfauna von Mitteleuropa 8/3). Heidelberg: Spektrum Akademischer Verlag.
Mezquita F and Miracle MR (1997) Chydorid assemblages in the sedimentary sequence of Lake La Cruz (Spain) subject to water level changes. *Hydrobiologia* 360: 277–285.
Mezquita F, Roca JR, Reed JM et al. (2005) Quantifying species-environment for ecological and paleoecological studies: Examples using Iberian data. *Palaeogeography, Palaeoclimatology, Palaeoecology* 225: 93–117.
Miracle MR (1978) Organització del zooplàncton d'aigua dolça durant un cicle anual: Aplicació d'un índex de fluctuacions. *Col loquis de la Societat Catalana de Biologia* 10: 183–193.
Miracle MR, Brito JM, Burjachs F et al. (2013) A multiproxy record of human mediated trophic and salinity changes in a coastal lagoon. In review.
Müller G (1968) Exceptionally high strontium concentrations in fresh water oncolites and mollusk shells of lake Constance. In: Miller G and Friedman GM (eds) *Recent Developments in Carbonate Sedimentology in Central Europe*. Berlin-Heidelberg-New York: Springer, pp. 116–127.
Müller G (1969) High strontium contents and Sr/Ca ratios in Lake Constance waters and carbonate and their sources in the drainage area of the Rhine River (Alpenrhein). *Mineral Deposita* 4: 75–84.
Peris-Albentosa T (1995) *La séquia Real del Xúquer (1258–1847) Síntesi històrica i aportacions medioambietals*. Alzira: Germania.
Poquet JM, Mezquita F, Rueda J et al. (2008) Loss of Ostracoda biodiversity in Western Mediterranean wetlands. *Aquatic Conservation: Marine and Freshwater Ecosystems* 18: 280–296.
Primavera M, Simone O, Fiorentino G et al. (2011) The palaeoenvironmental study of the Alimini Piccolo lake enables a reconstruction of Holocene sea-level changes in southeast Italy. *The Holocene* 21(4): 553–563.
Reed JM, Mesquita-Joanes F and Griffiths HI (2012) Multi-indicator conductivity transfer functions for Quaternary palaeoclimate reconstruction. *Journal of Paleolimnology* 47: 251–275.
Renard M (1985) Géochimie des carbonates pèlagiques. *Documents de Bureau des Recherches Géologiques et Mineralogiques* 85: 1–650.
Robles F, Collado MA and Borredá V (1985) Variaciones en la fauna de moluscos en la Albufera de Valencia: Implicaciones paleogeográficas. In: Homenaje a Juan Cuerda *Pleistoceno y Geomorfología litoral*. Universidad de Valencia, pp. 123–133.
Rodrigo MA, Alonso-Guillén JL, Cirujano S et al. (2009) Aproximación a las comunidades de carófitos que existieron en la Albufera de Valencia a partir del estudio de las oósporas del sedimento. *Anales del Jardín Botánico de Madrid* 66(2): 195–208.
Romo S, Villena MJ, Sahuquillo M et al. (2005) Response of a shallow Mediterranean lake to nutrient diversion: Does it follow similar patterns as in northern shallow lakes? *Freshwater Biology* 50(10): 1706–1717.
Ruiz F, Abad M, Caceres LM et al. (2010) Ostracods as tsunami tracers in Holocene sequences. *Quaternary Research* 73(1): 130–135.
Ruiz F, Abad M, Galán E et al. (2006) The present environmental scenario of El Melah Lagoon (NE Tunisia) and its evolution to a future sabkha. *Journal of African Earth Sciences* 44: 289–302.
Ruiz F, González-Regalado ML, Baceta JI et al. (2000a) Los ostrácodos de la laguna de Venecia (NE de Italia). *Geobios* 33: 447–454.
Ruiz F, Gonález-Regalado ML, Baceta JI et al. (2000b) Comparative ecological analysis of the ostracod faunas from low and high-polluted southwestern Spanish estuaries: A multivariate approach. *Marine Micropaleontolgy* 40: 345–376.
Sanchís-Ibor C (2001) *Regadiu i canvi ambiental a l'Albufera de València*. Publicacions de la Universitat de València.
Sanjaume E, Segura F, López-García MJ et al. (1992) Recent sedimentation in Valencia Lagoon: Preliminary results. *Journal of Coastal Research* 8(3): 688–698.
Serra M, Miracle MR and Vicente E (1984) Interrelación entre los principales parámetros limnológicos de la Albufera de Valencia. *Limnetica* 1: 9–19.
Shannon CE and Weaver W (1963) *The Mathematical Theory of Communication*. Urbana: University of Illionis Press.
Soria JM (2006) Past, present and future of la Albufera of Valencia Natural Park. *Limnetica* 25: 135–142.
Soria JM, Miracle MR and Vicente E (1987) Aporte de nutrientes y eutrofización de la Albufera de Valencia. *Limnetica* 3: 227–242.
Talbot MR (1990) A review of the palaeohydrological interpretation of carbon and oxygen isotopic ratios in primary lacustrine carbonates. *Chemical Geology* 80: 261–279.
Van Harten D (1975) Size and environmental salinity in the modern euryhaline ostracod *Cyprideis torosa* (Jones, 1850) a biometrical study. *Palaeogeography, Palaeoclimatology, Palaeogeography* 17: 35–48.
Vesper B (1972a) Zur Morphologie und Ökologie von *Cyprideis torosa* (Jones, 1850) (Crustacea, Ostracoda, Cytheridae) unter besonderer Berücksichtigung seiner Biometrie. *Mitteilungen Hamburger Zoologisches Museum und Institut* 68: 21–77.
Vesper B (1972b) Zum Problem der Buckelbildung bei *Cyprideis torosa* (Jones 1850) (Crustacea, Ostracoda, Cytheridae). *Mitteilungen Hamburger Zoologisches Museum und Institut* 68: 79–94.
Vicente E and Miracle MR (1992) The coastal lagoon Albufera de Valencia: An ecosystem under stress. *Limnetica* 8: 87–100.
Weinbauer MG and Velimirov B (1995) Calcium, magnesium and strontium concentrations in the calcite sclerites of Mediterranean gorgonians (Coelenterata: Octocorallia). *Estuarine, Coastal and Shelf Science* 40: 87–104.
Wetzel RG (1983) *Limnology*. 2nd edition. New York: Saunders College Publishing.
Whatley RC (1983) The application of ostracoda to paleoenvironmental analysis. In: Maddocks RF (ed.) *Applications of Ostracoda*. Houston: Department of Geosciences of the University of Houston, pp. 51–57.